# Molecular Structures of a Monovalent and a Divalent Nickel Catenate: Competition between Metal Orbital Requirements and Geometrical Constraints Imposed by the Ligand

Christiane O. Dietrich-Buchecker,[†] Jean Guilhem,[‡] Jean-Marc Kern,[†] Claudine Pascard,[*,‡] and Jean-Pierre Sauvage[*,†]

Laboratoire de Chimie Organo-Minérale, UA 422 au CNRS, Faculté de Chimie, Université Louis Pasteur, 67000 Strasbourg, France, and Laboratoire de Cristallochimie, Institut de Chimie des Substances Naturelles, CNRS, 91198 Gif-sur-Yvette-Cedex, France

Nickel(I) and nickel(II) catenates were crystallized, and their X-ray structures were solved. Ni(I) complex: $[C_{68}H_{68}N_4O_{12}Ni^+][ClO_4^-]\cdot C_6H_6\cdot CH_2Cl_2$, $a = 17.328(7)$ Å, $b = 14.965(6)$ Å, $c = 14.675(6)$ Å, $\alpha = 97.78(6)°$, $\beta = 111.46(8)°$, $\gamma = 97.84(5)°$, $V = 3481$ Å$^3$, triclinic $P\bar{1}$, $Z = 2$. Ni(II) complex: $[C_{68}H_{68}N_4O_{12}Ni^{2+}][BF_4^-]_2\cdot {}^1/_2C_6H_6\cdot {}^1/_2H_2O$, $a = 20.472(10)$ Å, $b = 24.255(8)$ Å, $c = 15.405(8)$ Å, $\beta = 113.80(2)°$, $V = 6999$ Å$^3$, monoclinic $C2/c$, $Z = 4$. The complexes consist of two interlocking 30-membered rings with two 2,9-diphenyl-1,10-phenanthroline fragments as coordinating units, complexed to mono- or divalent nickel. The extremely strong stabilization of Ni(I) as determined by electrochemistry (Ni(II)/Ni(I): $E° = -0.18$ V vs SCE in $CH_3CN$) is reflected by both structures. The ligand system is perfectly well adapted to a tetrahedral geometry as preferred by monovalent nickel and in agreement with the molecular structure found. On the other hand, the divalent state leads to a strongly distorted structure, in accordance with a d$^8$ configuration which is not likely to easily accommodate a tetrahedral environment. Rather, the geometry of the Ni(II) catenate is close to that of a square bipyramid lacking an axial position. Accordingly, the two chelate planes of the Ni(I) catenate being perpendicular to one another, no intramolecular stacking interactions between aromatic groups are observed, whereas in the Ni(II) case strong Π–Π interactions between phenyl rings and aromatic nuclei are present.

X-ray structures of nickel(I) complexes are relatively rare.[1] Macrocyclic systems allow a good control of the coordination sphere around the metal. A recent report dealt with a (thiaporphyrin)nickel(I) complex,[2] the corresponding nickel(II) compound being 5-coordinate due to the flat structure of the macrocyle, thus allowing additional ligands like Cl$^-$ to find access and bind to the metal.

Other examples include macrocyclic complexes consisting of substituted tetraazacyclotetradeca-4,11-diene[3] or containing a saturated cyclam-type ligand.[4] In the latter case, since the X-ray structures of the corresponding nickel(II) complexes were also known,[5] a direct comparison between Ni(I) and Ni(II) geometries could be made.[4] Although slight differences were noticed, with in particular two sets of Ni(I)–N bond distances as opposed to the analogous divalent nickel complexes which only contain one type of Ni–N bond ($d = 1.92$ Å), the molecular structures were basically the same. This similarity can easily be understood by considering the geometrical ligand requirements. The macrocycles used were 16-membered rings, and they display a very strong tendency to adopt square planar conformations when complexed to a transition metal. This is indeed what was observed, with only a small shift of Ni(I or II) or N positions from the average plane made by the four coordinating nitrogens. In these examples, the macrocyclic ligand imposes a square-planar geometry, regardless of the electronic properties of the metal center and, in particular, of the geometry of its most stable coordination polyhedron.

A [2]catenand,[6,7] consisting of two interlocking rings incorporating dpp subunits (dpp = 2,9-diphenyl-1,10-phenanthroline), contains four nitrogen atoms. Contrary to a cyclam-type ligand structure, the four coordination sites can be disposed in a pseudo-tetrahedral arrangement.[8] In addition, the ligand should have much more freedom than a monocycle to adopt various geometries and to position the nitrogen atoms around the metal center. Such a situation should better reflect the effect of the oxidation state on the complex structure than the case with a monocyclic organic backbone.

We now report the X-ray structures of four-coordinate nickel(I) and nickel(II) catenates, in relation to the electrochemical properties of the system. The chemical formulae of the ligands and the complexes are represented in Figure 1.

## Results and Discussion

**Synthesis, Electrochemistry, and UV–Vis and EPR Spectroscopy.** The nickel(II) catenate $[1\cdot Ni^{2+}][BF_4^-]_2$ was prepared from $Ni(NO_3)_2\cdot 6H_2O$ and **1** in $CH_3OH/CH_2Cl_2$ (2:1) followed by anion exchange. It was obtained as a dark orange solid in 52% yield. The monovalent nickel(I) complex was generated by electrochemical reduction of the nickel(II) catenate (−0.45 V vs SCE in $CH_3CN$). It was crystallized from $CH_2Cl_2$/benzene.

As previously discussed,[9,10] the monovalent state is greatly stabilized by the catenate structure. The determining factor is

† Université Louis Pasteur.
‡ Institut de Chimie des Substances Naturelles.
® Abstract published in *Advance ACS Abstracts*, July 1, 1994.
(1) Nag, K.; Chakravorty, A. *Coord. Chem. Rev.* **1980**, *33*, 87–147 and references cited therein.
(2) Latos-Grazynski, L.; Olmstead, M. M.; Balch, A. L. *J. Am. Chem. Soc.* **1989**, *28*, 4065–4066.
(3) Furenlid, L. R.; Renner, M. W.; Szalda, D. J.; Fujita, E. *J. Am. Chem. Soc.* **1991**, *113*, 883–892.
(4) Suh, M. P.; Kim, H. K.; Kim, M. J.; Oh, K. Y. *Inorg. Chem.* **1992**, *31*, 3620–3625.
(5) Suh, M. P.; Kang, S.-G.; Goedken, V. L.; Park, S.-H. *Inorg. Chem.* **1991**, *30*, 365–370.

(6) Dietrich-Buchecker, C. O.; Sauvage, J.-P.; Kern, J.-M. *J. Am. Chem. Soc.* **1984**, *106*, 3043–3045. Dietrich-Buchecker, C. O.; Sauvage, J.-P. *Tetrahedron* **1990**, *46*, 503–512.
(7) Sauvage, J.-P. *Acc. Chem. Res.* **1990**, *23*, 319–327. Dietrich-Buchecker, C. O.; Sauvage, J.-P. *Bioorganic Chem. Frontiers* **1991**, *2*, 195–248.
(8) Cesario, M.; Dietrich-Buchecker, C. O.; Guilhem, J.; Pascard, C.; Sauvage, J.-P. *J. Chem. Soc., Chem. Commun.* **1985**, 244–247.
(9) Dietrich-Buchecker, C. O.; Kern, J.-M.; Sauvage, J.-P. *J. Chem. Soc., Chem. Commun.* **1985**, 760–762.
(10) Dietrich-Buchecker, C. O.; Sauvage, J.-P.; Kern, J.-M. *J. Am. Chem. Soc.* **1989**, *111*, 7791–7800.
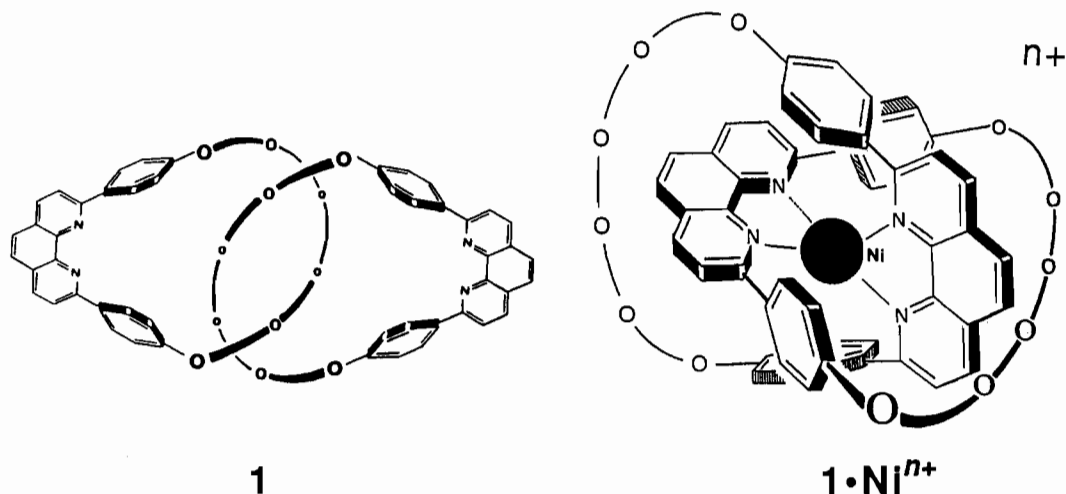
**Figure 1.** Representation of the catenand and its nickel complex. The oxygen atoms of the catenand are linked by $-CH_2-CH_2-$ units.

the geometry of the complex formed by entwining two dpp subunits around a nickel center. In this way a square-planar situation is strictly prohibited due to the presence of the aromatic substituents $\alpha$ to the nitrogen atoms of the phenanthroline nuclei. The spectacular stabilization of the +1 oxidation state can thus be explained in two ways by considering the 3d orbitals:

(i) Nickel(II) complexes are very generally planar since, for a $d^8$ configuration, the strongly antibonding orbital $2b_{1g}$ originating from $d_{x^2-y^2}$ is vacant, the 8 electrons occupying the 4 other low-lying orbitals $b_{2g}$, $e_g$, and $2a_{1g}$.[11,12]

By contrast, in tetrahedral coordination, occupation of antibonding orbitals ($t_2$) cannot be avoided and tends to destabilize the complex, which corresponds to the present situation. (ii) The $d^9$ electronic configuration of monovalent nickel is in complete opposition with a $D_{4h}$ geometry since the high-lying antibonding orbital $2b_{1g}$ ($d_{x^2-y^2}$) would now have to be occupied. On the contrary, in a tetrahedral situation, the addition of one electron to the $d^8$ metal will not imply such a dramatic change as for $D_{4h}$ coordination since $t_2$ levels are already occupied.

The overall effect of the factors discussed in (i) and (ii) is to strongly favor tetrahedral monovalent nickel. This is remarkably illustrated by the electrochemical properties of $1 \cdot Ni^{n+}$. For a square-planar tetraaza complex, the redox potential of the $Ni^{II/I}$ couple is typically around $-1.3$ V vs SCE in $CH_3CN$.[4] For the nickel catenate, this value is shifted by more than 1 V: $E° = -0.18$ V for $1 \cdot Ni^{2+/+}$. It is even possible to reduce the monovalent complex to the neutral species without any decomposition, as evidenced by the reversible cyclic voltammogram given in Figure 2. The second reduction process $1 \cdot Ni^{+/0}$ occurs at $E° = -1.325$ V.

The nickel(II) catenate is paramagnetic, in agreement with its non-square-planar geometry. As already noticed,[10] the EPR spectrum of $1 \cdot Ni^+$ is typical for a $d^9$ electronic configuration, although more information regarding the coordination geometry of the metal is difficult to obtain from the three $g$ values. The EPR spectrum of $1 \cdot Ni^+$ in frozen $CH_2Cl_2$ solution is indicated in Figure 3.

The electronic spectra of the compounds $1 \cdot Ni^{n+}$ ($n = 2, 1$) show the expected intense bands in the UV region associated with the aromatic dpp fragments. More interesting is the visible region. $1 \cdot Ni^{2+}$ is a deep orange complex, with a relatively intense d–d band in the visible ($\lambda_{max} \sim 480$ nm, $\epsilon \sim 450$). The position of this band is indicative of a distorted geometry.[12] The nickel(I) catenate is an intensely colored complex. The crystals are deep

(11) Albright, T. A.; Burdett, J. K.; Whangbo, M.-H. *Orbital Interactions in Chemistry*; J. Wiley and Sons: New York, 1986.
(12) Cotton, F. A.; Wilkinson, G. *Advanced Inorganic Chemistry*, 5th ed.; J. Wiley and Sons: New York, 1988; pp 743–755.
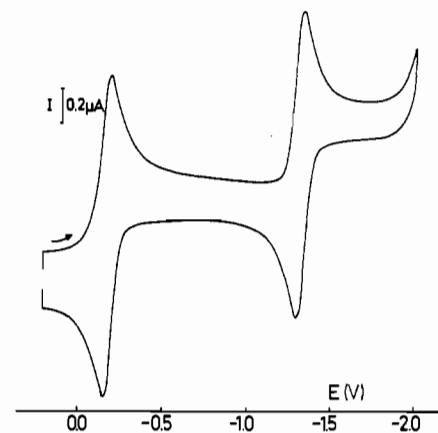
**Figure 2.** Cyclic voltammetry of $1 \cdot Ni^{2+}$ in $CH_3CN$ at room temperature. Supporting electrolyte: 0.1 mol·L$^{-1}$ TEAP. Scan rate: 50 mV·s$^{-1}$; $E$ versus SCE.



$g_1 = 2.388$

$g_2 = 2.143$

$g_3 = 2.071$
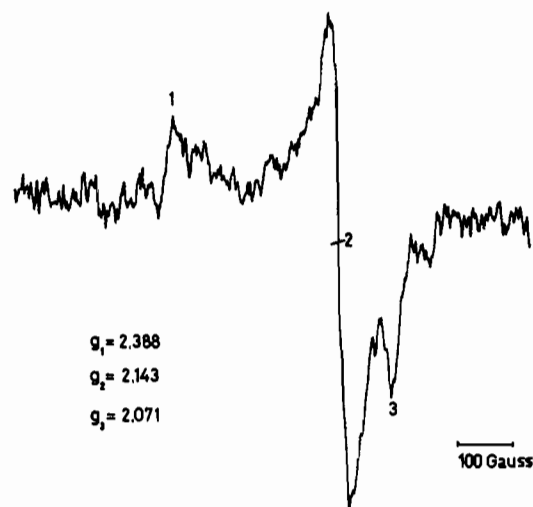
**Figure 3.** EPR spectrum of $1 \cdot Ni^+$ ($2.2 \times 10^{-4}$ mol·L$^{-1}$ in 0.1 mol·L$^{-1}$ $CH_2Cl_2$/TEAP; frozen solution).

blue, and the visible spectrum in solution shows a broad band centered at 645 nm ($\epsilon \sim 4800$). This band is likely to correspond to a metal-to-ligand charge-transfer transition from the electron-rich metal center to the accessible $\Pi^*$ levels of the phen ring (phen = 1,10-phenanthroline). This strong absorption precludes observation of metal-centered electronic transitions.

**Molecular Structures of $[1 \cdot Ni^+][ClO_4^-]$ and $[1 \cdot Ni^{2+}][BF_4^-]_2$.** The molecular structure of the nickel(I) catenate is represented in Figure 4. As compared to that of the copper(I) catenate $1 \cdot Cu^+$,[9]

**Figure 4.** (a) Top: Ortep representation of the nickel(I) catenate. The plane of PhenA is taken as plane of projection. PhenA is within the black line. (b) Bottom: Stereographic view of the nickel(I) catenate. The figure is rotated 90° with respect to (a) so that PhenA (now in white) is seen nearly perpendicular to the paper.

**Table 1.** Coordination Polyhedron around the Copper or Nickel Centers: $N_x \cdots N_y$ Distance (Å) and $[N_x, M^+, N_y]$ angle (deg)

| $N_x$ | $N_y$ | Cu(I) | Ni(I)[a] | Ni(II)[b] |
|-------|-------|-------|----------|-----------|
| N1A   | N10B  | 3.7 [130] | 3.8 [142] | 3.6 [124] |
| N10A  | N1B   | 3.7 [130] | 3.6 [135] | 3.6 [124] |
| N1A   | N1B   | 3.7 [137] | 3.2 [108] | 2.8 [86.5] |
| N10A  | N10B  | 2.9 [88]  | 3.3 [111] | 3.7 [141] |
| N1A   | N10A  |           | [84.6]    | [86.5] |
| N1B   | N10B  |           | [84.8]    | [86.5] |

[a] Atom numbering in B ring should be permuted to coincide with Cu(I) catenate (i.e. N1B and N10B and vice versa). [b] Atom numbering should be completely inverted with N1A as N10A and N1B as N10B to compare with the other structures.

it is much more regular. The coordination polyhedron around Ni(I) is significantly less distorted (Figure 4b) than Cu(I). Whereas the copper center is situated asymmetrically with respect to its 4 coordinated nitrogens, the lengths of the N–N edges of the Ni(I) coordination tetrahedron are divided into 2 pairs of values. Table 1 compares the numerical values of the coordination tetrahedron around the cation center for the two catenates of Cu(I) and Ni(I).

Very few Ni(I) complexes with all-nitrogen ligands are known, and it is thus difficult to compare the present compound with previous structures. In the factor 430 model (hydrocorphin replaced by another 16-membered ring incorporating two N=C double bonds) proposed by Furenlid et al.[3] two sets of Ni(I)–N distances have been found: Ni(I)–$N_{amine}$ = 1.98(1) Å and Ni-(I)–$N_{imine}$ = 2.06(1) Å. These distances have been confirmed by EXAFS experiments. They are larger than the Ni(II)–N distances (1.92(1) Å) found in another macrocyclic structure, the Ni(II)–isobacteriochlorin complex.[13]

The solid-state study of the Ni(I) catenate shows, for the first time to our knowledge, a tetrahedral environment of Ni(I) (see Table 2b). The Ni(I)–N distances observed range from 1.96 to 2.01 Å with an average of 1.98(2) Å, in agreement with the above previously published values (see Table 2a).

(13) Renner, M. W.; Furenlid, L. R.; Barkigia, K. M.; Forman, A.; Shim, H.-K.; Simpson, D. J.; Smith, K. M.; Fajer, J. *J. Am. Chem. Soc.* **1991**, *113*, 6891–6898.

**Table 2.** Distances (Å) and Angles (deg) for the Ni Complexes

| | $1 \cdot Ni^+$ | $1 \cdot Ni^{2+}$ |
|---|---|---|
| (a) Nickel $\cdots$ Phenanthroline Nitrogen Distances[a] | | |
| Ni$\cdots$N1A | 1.978(2) | 1.97(1) |
| Ni$\cdots$N10A | 1.964(11) | 2.05(1) |
| Ni$\cdots$N1B | 1.958(11) | 1.97(1) |
| Ni$\cdots$N10B | 2.015(9) | 2.05(1) |
| average | 1.98 ± 0.02 | 2.01 ± 0.04 |
| (b) Valency Angles around Nickel | | |
| N1A, N10B | 142.9(5) | 124(1) |
| N1B, N10A | 136.1(6) | 124(1) |
| N1B, N10B | 84.8(5) | 86(1) |
| N1A, N10A | 84.6(5) | 86(1) |
| N1A, N1B | 107.8(6) | 87(1) |
| N10A, N10B | 110.7(5) | 140(1) |

[a] Average $\langle N \cdots Cu(I) \rangle$: 2.05 + 0.03 Å.

The structure of the divalent nickel catenate $1 \cdot Ni^{2+}$ is depicted in Figure 5 as well as the metal coordination polyhedron. Some important bond distances and angles are collected in Tables 1 and 2. The nickel(II) atom is located on a binary axis. The molecule is directly comparable to $1 \cdot Cu^+$ [8] with a dihedral angle between the two phenanthroline units of 65°. The most striking aspect comes from the gliding of one phenanthroline under the mean plane of the second phenanthroline, the torsion of the two units being then absolutely identical to $1 \cdot Cu^+$ spatial structures. This is seen by the short distance (and the low angle value) between two nitrogens of the two opposed units (Table 1). Consequently, the opposed angle is very open (140°) with a larger N–N distance (3.7 Å). The nickel atom is practically in the plane of three of the nitrogen atoms (0.33 Å below the triangle plane N1B, N10A, N10B). Very different is the situation for $1 \cdot Ni^+$. The nitrogen atom polyhedron of $1 \cdot Ni^+$ is symmetrical, (see Table 2b), the two phenanthroline nuclei being disposed in a less distorted fashion. This regular geometry of the complex makes the metal center more protected than in the divalent complex. In the latter case, the nickel atom is relatively accessible, which could perhaps allow a fifth ligand to find access and coordinate the metal under particular circumstances, whereas this seems to be very unlikely in the monovalent nickel complex.
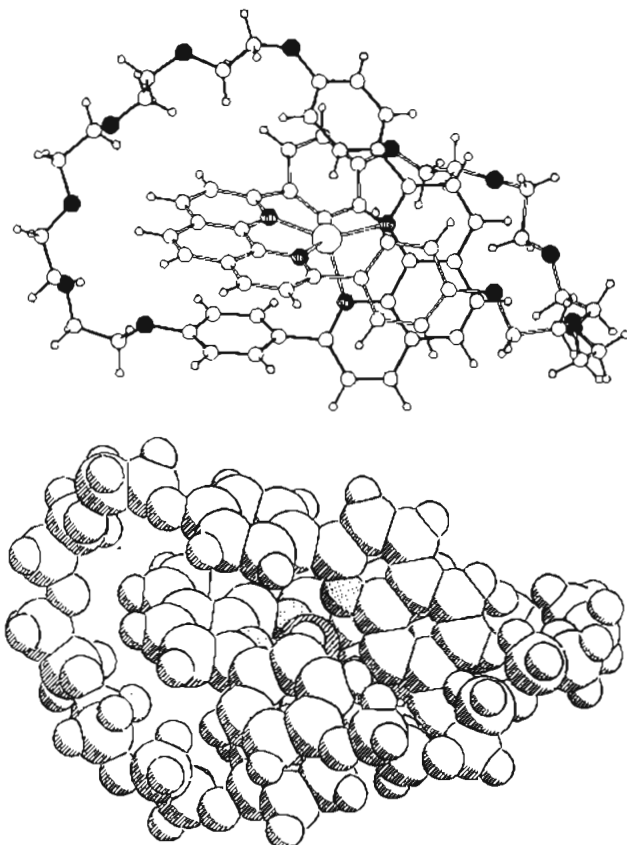
**Figure 5.** (a) Top: Ortep representation of the nickel(II) catenate with the same orientation as for 1·Ni⁺ in Figure 4a. (b) Bottom: CPK drawing of 1·Ni⁺.
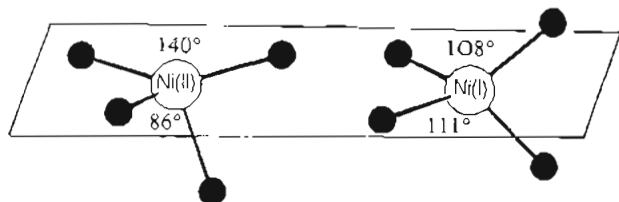


**Figure 6.** Coordination around the metal center: left, divalent nickel (1·Ni²⁺); right, monovalent nickel (1·Ni⁺).

The geometry difference between the two nickel catenates is striking, and it is in perfect accordance with the electronic factors discussed above. For comparison, the coordination polyhedra of 1·Ni⁺ and 1·Ni²⁺ are represented in Figure 6. As already mentionned, the d⁹ configuration is such that the tetrahedral situation is preferred to the square-planar one for a monovalent metal complex, in spite of conformational preferences of the ligand. This is well illustrated by the fact that, in 1·Ni⁺, no stacking interactions are observed contrary to all the other catenates studied.[8,14,15] The stabilizing Π–Π interaction found between the donor anisyl-type nucleus and the electron-accepting phenanthroline unit of the other ring as observed in 1·Cu⁺, for instance, implies an asymmetrical structure for the molecule with, in particular, a strongly distorted geometry around the metal. This distorsion would cost too much energy in 1·Ni⁺ as compared to the small energy gain brought by the stacking. The monovalent nickel center imposes a tetrahedral geometry (or, at least, a symmetrical arrangement) at the expense of the organic backbone. Not only are the Π–Π interactions inhibited but, even more, the

(14) Cesario, M.; Dietrich-Buchecker, C. O.; Edel, A.; Guilhem, J.; Kintzinger, J.-P.; Pascard, C.; Sauvage, J.-P. *J. Am. Chem. Soc.* **1986**, *108*, 6250–6254.

(15) Dietrich-Buchecker, C. O.; Guilhem, J.; Khemiss, A. K.; Kintzinger, J.-P.; Pascard, C.; Sauvage, J.-P. *Angew. Chem., Int. Ed. Engl.* **1987**, *26*, 661–663.

**Table 3.** Comparison between Cu(I), Ni(I), and Ni(II) Catenates

Dihedral Angles (deg) of the Aromatic Planes of
Two Different Complexed Units A and B

|  |  | Cu(I) | Ni(I) | Ni(II) |
|---|---|---|---|---|
| PhenA | Ph2B | 6 | 15 (Ph1B) | 5 |
| PhenB | Ph2A | 11 | 15 | 5 |
| Ph1A | Ph1B | 5 | 35 (Ph2B) | 6 |
| PhenA | PhenB | 60.6 | 62.7 | 63.4 |

Dihedral Angles (deg) between
the Planes Belonging to the Same Unit[a]

|  |  | Cu(I) | Ni(I) | Ni(II) |
|---|---|---|---|---|
| PhenA | Ph1A | 55 | 47 | 60 |
| PhenA | Ph2A | 52 | 52 | 41 |
| PhenB | Ph1B | 27 | 33 (Ph2B) | 60 |
| PhenB | Ph2B | 58 | 52 (Ph1B) | 41 |

Dihedral Angles (deg) between
All Aromatic Planes for Nickel Catenates

|  |  | angle I, II | |
|---|---|---|---|
| I | II | Ni(I) | Ni(II) |
| PhenA | Ph1B | 15 | 5 |
|  | Ph2B | 42 |  |
| PhenB | Ph1A | 21 |  |
|  | Ph2A | 15 | 5 |
| Ph1A | Ph1B | 34 |  |
| Ph2A | Ph2B | 17 | 6 |

Deviations (Å) from Aromatic Mean Planes[b] for Ni(I) Catenate

| | Ph1A | Ph1B | | Ph2A | Ph2B |
|---|---|---|---|---|---|
| C15 | +0.050 (4δ) | −0.012 (3δ) | C37 | −0.035 (4δ) | 0.055 (3δ) |
| C16* | +0.014 | −0.004 | C38* | +0.008 | +0.020 |
| C17* | −0.014 | +0.004 | C39* | −0.008 | −0.020 |
| C18 | +0.119 (9δ) | −0.020 (5δ) | C40 | −0.070 (9δ) | +0.063 (3δ) |
| C19* | +0.014 | −0.004 | C41* | +0.008 | +0.020 |
| C20* | −0.014 | +0.004 | C42* | −0.008 | −0.020 |
| O21A | +0.297 (21δ) | −0.166 (41δ) | O36 | −0.166 (21δ) | −0.078 (4δ) |

[a] This goes along with more or less rotation of the phenyl rings around their link to the phenanthrolines. [b] Atoms with an asterisk are included in the plane computation. For the others, the distance is compared with the average value.

aromatic rings attached to the phenanthroline nuclei are bent. In Table 3 are given some important geometrical data regarding the aromatic nuclei arrangement (dihedral angles between aromatic planes) and deviations from the mean planes of the bent aromatic nuclei.

It is noteworthy that by oxidizing Ni(I) to Ni(II) the coordinated phen nuclei become significantly more electron deficient and thus are prompted to undergo acceptor–donor stacking. As a consequence, the propensity of the compound to form intramolecular Π–Π stacks increases by oxidation. In other words, two distinct factors participate in favoring a stacked arrangement in 1·Ni²⁺: (i) The divalent nickel(II) center favors a strongly distorted geometry and (ii) this is in accordance with formation of acceptor–donor complexes between anisyl-type nuclei and phen subunits. Electronic factors common to both the metal and the ligands move in the same direction, i.e. toward strong distortion of the coordination tetrahedron, thus allowing intramolecular stacking interactions to take place. This tendency is clearly evidenced by the data of Table 3.

In copper(I) and nickel(II) catenates, the displacement of a phenanthroline from a symmetrical position provides a maximum of overlapping between aromatic rings, which results in superimposition of each phenanthroline with one phenyl, with small dihedral angles (3–11°).

The best superimposition of aromatic parts occurs in 1·Ni²⁺ with complete overlap of a phenyl and a phenanthroline at 3.2-Å distance.

In the more symmetrical geometry of the nickel(I) catenate, each phenanthroline is pinched between the two phenyl rings

**Table 4.** Crystallographic Data for Ni(I) and Ni(II) Catenates

| | Ni(I) | Ni(II) |
|---|---|---|
| formula | $[C_{68}H_{68}N_4O_{12}Ni^+][ClO_4^-]\cdot$ $C_6H_6\cdot CH_2Cl_2$ | $[C_{68}H_{68}N_4O_{12}Ni^{2+}][BF_4^-]_2\cdot$ $^1/_2C_6H_6\cdot^1/_2H_2O$ |
| fw | 1453.2 | 1408.7 |
| system | triclinic | monoclinic |
| group | $P\bar{1}$ | $C2/c$ |
| cryst, mm$^3$ | prism, 0.4 × 0.2 × 0.1 | prism, 0.2 × 0.2 × 0.2 |
| $a$, Å | 17.328(7) | 20.472(10) |
| $b$, Å | 14.965(6) | 24.255(8) |
| $c$, Å | 14.675(6) | 15.405(8) |
| $\alpha$, deg | 97.78(6) | 90 |
| $\beta$, deg | 111.46(8) | 113.80(2) |
| $\gamma$, deg | 97.84(5) | 90 |
| $V$, Å$^3$ | 3481 | 6999 |
| $Z$ | 2 | 4 |
| $T$, °C | 21 | 21 |
| $\lambda$, Å | 0.7107 (Mo K$\alpha$) | 1.5418 (Cu K$\alpha$) |
| $\mu$, cm$^{-1}$ | 4.2 | 1.05 |
| $\rho_{cal}$, g cm$^{-3}$ | 1.38 | 1.34 |
| $\rho_{obs}$ | not measd | not measd |
| $R(F_o)$,$^a$ % | 8.3 | 12.5 |
| $R_w(F_o)$,$^b$ % | 9.0 | 12.9 |

$^a R = [\Sigma(F_o - F_c)^2/\Sigma F_o^2]$. $^b R_w = [\Sigma w(F_o - F_c)^2/\Sigma wF_o^2]^{1/2}$.

bonded to the second Phen (see stereo drawing Figure 2 and Table 3), forming with them larger dihedral angles (15–42°). The linked phenyls cannot overlap as much as they would in a less symmetrical situation, and the created strain results in the aromatic plane deformation.[16]

On each side of PhenB, the phenyl rings Ph1A and Ph2A undergo a strong deformation: the bridge-head carbons, C15 and C18 in Ph1A and C37 and C40 in Ph2A, are out of the phenyl plane (see Table 3) giving to the aromatic ring a boat conformation, thus coming closer to the phenanthroline aromatic ring. Consequently, the two oxygen atoms, O21A and O36A, are nearer than geometrically expected: 8.7 Å vs 11 Å. Moreover, the arms bearing the two phenyl A groups seem to have moved up and down, so as to superimpose Ph1A above N1B and PH2A above N10B.

The two phenyl B rings stand on each side of Phen A. We notice the same deformation on Ph1B, bending toward PhenA but not on Ph2B (see Table 3). The latter ring is also associated with a strong tilt angle (42°) with respect to PhenA. We think the explanation lies in the proximity, in the crystal cell, of another Ph2B, centrosymmetrically related to the first one, face-to-face and at 4.00-Å distance. Thus there is a competition between internal interaction and external interaction, due to crystal packing. The parallel stacking is stronger than the interactive forces between inclined aromatic units.[17]

In the other structures the overlap of the phenyl and the phenanthroline is between two nearly parallel rings, and no real deformation was observed (as far as the precision goes).

In conclusion, the use of the highly flexible ligand 1, containing four nitrogen donor sites, allows one to prepare both monovalent and divalent nickel complexes. The electrochemical data and simple molecular orbital considerations are in good agreement, as well as the molecular structures determined by X-ray crystallography. It is interesting to notice that the geometry of the system is completely governed by the metal for the nickel(I) catenate (high symmetry, as close as possible from a tetrahedral arrangement), the ligand requirements being unsatisfied. By

(16) For a recent example of out-of-plane deformation in aromatic compounds, see: Saitmacher, K.; Schulz, J. E.; Nieer, M.; Vögtle, F. *J. Chem. Soc., Chem. Commun.* **1992**, 175–176.

(17) Hunter, C. A.; Sanders, J. K. M. *J. Am. Chem. Soc.* **1990**, *112*, 5525–5534.

(18) Sheldrick, G. M. Shelx76, Program for Crystal Structure Determination. University of Cambridge, United Kingdom.

contrast, in the divalent catenate **1·Ni$^{2+}$** both metal center *and* ligand seem to adopt a favorable geometrical arrangement, leading to a highly distorted metal polyhedron coordination but good intramolecular stacking interactions.

## Experimental Section

**Preparation of the Nickel(II) Complex. [Ni$^{II}$(Cat30)](BF$_4$)$_2$.** A large excess of Ni(NO$_3$)$_2$·6H$_2$O (72 mg; 0.25 mmol) in 10 mL of MeOH was added with stirring at room temperature to a solution of **1** (83 mg; 0.073 mmol) in 5 mL of CH$_2$Cl$_2$. The mixture turned rust brown instantaneously. The quite slow complex formation was followed by TLC (progressive disappearance of free catenand over 2 days). Thereafter, the solution was evaporated to dryness, and the crude compound was taken up in 50 mL of water and CH$_2$Cl$_2$ (1:1). The organic layer was washed with water in order to remove excess nickel salt, dried over MgSO$_4$, filtered, and evaporated to dryness. Unsuccessful recrystallization attempts in CH$_2$Cl$_2$/C$_6$H$_6$ led us to exchange NO$_3^-$ for BF$_4^-$ (stirring of [Ni (Cat 30)$^{2+}$][NO$_3^-$]$_2$ dissolved in CH$_2$Cl$_2$ and a trace of water in presence of a large excess of NaBF$_4$ overnight). The now bright orange organic layer was washed with water and dried over MgSO$_4$. The crude complex as its BF$_4^-$ salt could be recrystallized in CH$_2$Cl$_2$/C$_6$H$_6$, affording an analytical sample (52 mg; 52% yield).

**[Ni$^{II}$(Cat30)][BF$_4^-$]$_2$.** Dark orange crystals formed, mp 234–235 °C. Anal. Calcd for C$_{68}$H$_{68}$N$_4$O$_{12}$NiB$_2$F$_8$: C, 59.80; H, 5.02; N, 4.10. Found: C, 59.79; H, 4.84; N, 4.01. UV–vis [$\lambda_{max}$ (log $\epsilon$)]: 228 (4.72), 250 (4.62), 318 (4.46), sh 480 (2.6).

**Preparation and Crystallization of [Ni(Cat30)][ClO$_4$].** A gastight cell with two compartments divided by a G3 sintered glass frit was used. The two compartments were externally connected by a two-ended needle to avoid the occurence of over-pressure phenomena during the electrolysis. Platinum wires were used as counter and working electrodes ($S$ = 23 cm$^2$ for the working electrode). A SCE reference electrode was connected to the cathodic compartment through an electrolytic junction (0.1 mol·L$^{-1}$ CH$_3$CN/(TEA)BF$_4$).

A 28-mg amount (0.02 mmol) of [Ni(Cat 30)][BF$_4$]$_2$ was dissolved in 20 mL of 0.1 mol·L$^{-1}$ CH$_3$CN/LiClO$_4$. After the solution was thoroughly deaerated with argon, electrolysis was performed at –0.45 V vs SCE, until the theoretical amount of current was consumed. The solution became dark-blue. The catholyte solution was transferred under vacuum (double-ended needle technique) into a Schlenk-type flask and the solvent evacuated under vacuum. Successively, 20 and 5 mL of degassed CH$_2$Cl$_2$ and H$_2$O were introduced into the Schlenk flask. After dissolution of LiClO$_4$ into the water layer, the organic phase was pumped and filtered, under reduced pressure, over degassed MgSO$_4$ into a gastight flask. The solvent was partially evacuated, and deareated benzene was added in such a quantity that the limit of solubility of the nickel salt was not reached. Blue-black crystals of [Ni(Cat30)][ClO$_4$] appeared after a few days.

**Crystal Structure Determinations.** Both crystals were mounted in a glass capillary to prevent solvent loss and mounted on a 4-circle automatic diffractometer. The crystallographic data are listed in Table 4.

**Nickel I.** The structure was solved by Patterson methods and refined with the large blocks least-squares (Sheldrick)[18] method, using anisotropic thermal parameters for heteroatoms, with the exception of the disordered ones. The molecule of the solvent were located in the asymmetric unit. The hydrogen atoms were calculated at their theoretical positions (C–H = 1 Å).

The catenate lies on a diad axis passing through the nickel atom. The two anions are disordered, and the benzene molecule is situated on the same binary axis with an occupation factor of one-half. The atomic parameters were refined with the full-matrix method using rigid blocks for the aromatic units and were kept isotropic except for nickel, oxygen, and nitrogen atoms. The high value of the $R$-factor is explained by the low number of observed reflections for the number of refined parameters. All the crystallographic data are given in Table 4.